2007

Ultrastructure of Teliospores and Promycelium and Basidiospore Formation in the Four-Spored Form of Gymnoconia Nitens, One of the Causes of Orange Rust of Rubus

C. W. Mims

E. A. Richardson

Josephine Taylor
Stephen F Austin State University, Department of Biology, jtaylor@sfasu.edu

Ultrastructure of teliospores and promycelium and basidiospore formation in the four-spored form of *Gymnoconia nitens*, one of the causes of orange rust of *Rubus*

Charles W. Mims, Elizabeth A. Richardson, and Josephine Taylor

Abstract: Orange rust of *Rubus* is an interesting disease because of the fact that it can be caused by three different rust fungi that produce virtually identical symptoms. One is *Gymnoconia peckiana* (Howe in Peck) Trotter, which is a demicyclic species, while the other two are endocyclic forms historically referred to as *Gymnoconia nitens* (Schwein.) Kern & H.W. Thurston. Although the spores produced on infected *Rubus* leaves by these latter two forms are morphologically identical to the aeciospores of *G. peckiana*, they actually function as teliospores. However, the teliospores of one of the forms gives rise to two-celled promycelia that bear only two basidiospores, while teliospores of the other produce four-celled promycelia bearing four basidiospores. Here, we examined the teliospores of the four-spored form along with the sequence of events that lead to basidiospore development. Developing and mature teliospores were binucleate, and we saw no evidence that karyogamy occurred in these spores. Upon germination, both spore nuclei migrated into the promycelium and underwent mitosis to form a total of four nuclei. Four transverse septa then developed, creating four uninucleate cells. A tapered sterigma arose from each cell and gave rise to a basidiospore. These findings indicate that the basidiospores of the four-spored form of *G. nitens* were formed in an asexual fashion.

Key words: Uredinales, scanning electron microscopy, transmission electron microscopy.

Résumé : La rouille orangée du *Rubus* constitue une maladie intéressante, parce que trois champignons distincts de la rouille peuvent la causer, en produisant des symptômes presque identiques. Le premier, une espèce hémicyclique, appartient au *Gymnoconia peckiana* (Howe in Peck) Trotter, alors que l'on réfère historiquement les deux autres, possédant des formes endocycliques, au *Gymnoconia nitens* (Schwein.) Kern & H.W. Thurston. Bien que les spores produites par ces deux dernières formes, sur les feuilles infectées du *Rubus*, possèdent une morphologie identique à celle du *G. peckiana*, elles agissent plutôt comme des téliospores. Cependant, alors que les téliospores d'une de ces formes produisent des promycéliums à deux cellules ne portant que deux basidiospores, les téliospores de l'autre forme produisent des promycéliums à 4 cellules avec quatre basidiospores. Les auteurs ont examiné les téliospores de la forme à quatre spores, ainsi que la séquence des évènements qui conduisent au développement de la basidiospore. Les téliospores en développement et matures comportent deux noyaux et ne montrent aucune évidence de caryogamie dans ces spores. Pendant la germination, les deux noyaux des deux spores migrent dans le promycélium et subissent la mitose pour former un total de quatre noyaux. Quatre septations transverses se développent, formant quatre cellules uninucléées. Un stérigmate effilé apparaît sur chaque cellule pour donner naissance à la basidiospore. Ces observations indiquent que les basidiospores de la forme à quatre spores du *G. nitens* se forment de façon asexuée.

Mots-clés : Urédinales, microscopie électronique par balayage, microscopie électronique en transmission.

[Traduit par la Rédaction]

Introduction

Orange rust is an extremely common disease of both wild and cultivated blackberry (*Rubus* spp.) in the US, and has been studied at the level of light-microscopy by numerous early workers (Newcombe and Galloway 1890; Clinton 1893; Olive 1908; Kunkel 1913, 1914, 1916; Dodge 1924). The disease is very important in the northeastern US (Kleiner and Travis 1991), but is also widespread in the southern states. From a mycological standpoint, orange rust is particularly interesting because it can be caused by three different pathogens that produce virtually identical symptoms. One is *Gymnoconia peckiana* (Howe in Peck) Trotter, also known as *Arthuriomyces peckianus* (Howe in Peck) Cummins & Y. Hirats., which is demicyclic, while the other two are endocyclic forms historically referred to as *Gymnoconia nitens* (Schwein.) Kern & H.W. Thurston. However, according to Cummins and Hiratsuka (2003), neither of these the endocyclic forms has either a proper generic name or a legitimate epithet. All three of the pathogens noted

Received 2 August 2007. Published on the NRC Research Press Web site at canjbot.nrc.ca on 28 October 2007.

C.W. Mims.[1] Department of Plant Pathology, University of GA, Athens, GA 30602, USA.
E.A. Richardson. Department of Plant Biology, University of GA, Athens, GA 30602, USA.
J. Taylor. Department of Biology, Stephen F. Austin State University, Nacogdoches, TX 75962, USA.

[1]Corresponding author (e-mail: cwmims@uga.edu).

 doi:10.1139/B07-097

Figs. 1–3. Leaves of *Rubus trivialis* infected by *Gymnoconia nitens*. Fig. 1. Leaves whose undersides are covered with sori (near-actual size). Figs. 2 and 3. Sori viewed using a dissecting microscope. Scale bars = 0.5 mm.

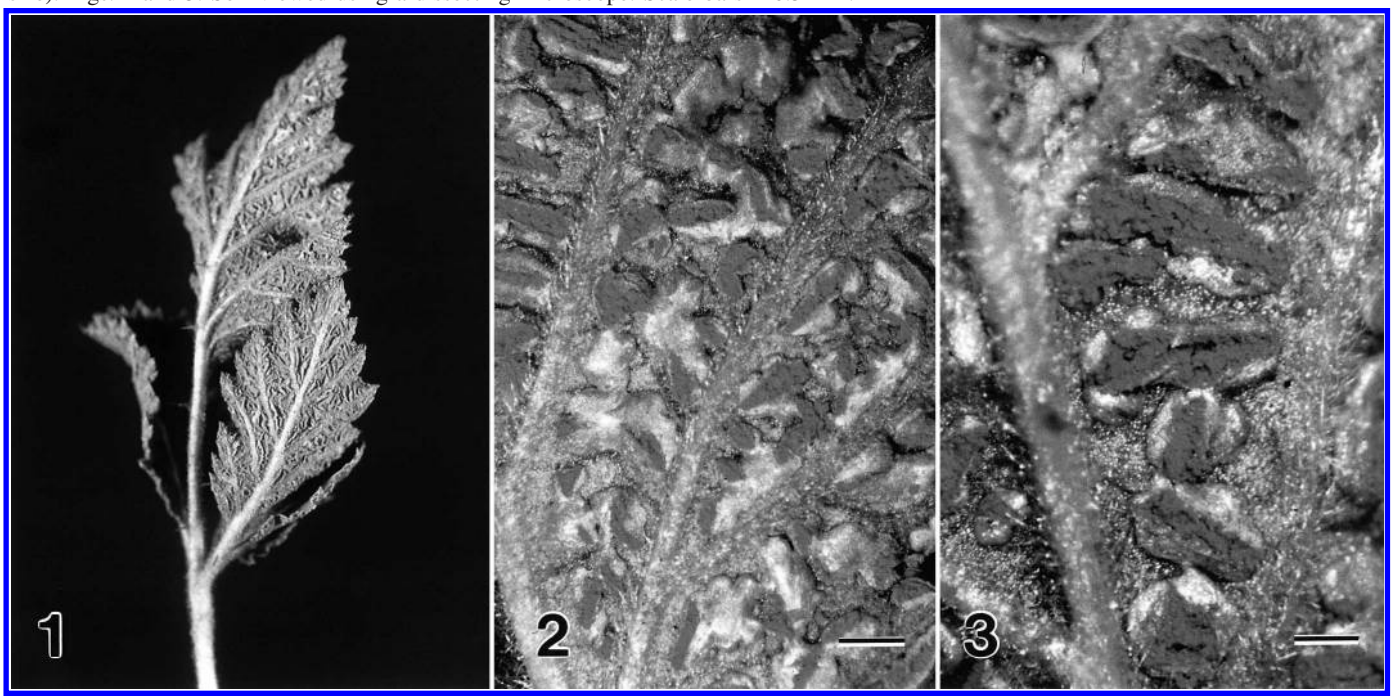

above are autoecious rusts that cause permanent, systemic infections involving blackberry roots. Each spring, crowns on infected roots give rise to weak, spindly shoots with typically stunted and pale-green leaves whose undersides become bright orange as the result of the development of tremendous numbers of sori filled with spores (Kunkel 1916; Dodge 1924; Kleiner and Travis 1991). In the case of *G. peckiana*, these spores are aeciospores, but in the two endocyclic forms they are actually caeomatoid teliospores (i.e., spores that are formed in the same manner as the aeciospores of the anamorphic rust genus *Caeoma* but which function as teliospores). The study of orange-rust disease becomes even more complicated because the two endocyclic forms, both referred to hereinafter as *G. nitens*, were likely confused with one another prior to 1924 (Dodge 1924). One of these forms possesses spermogonia and produces four-celled promycelia and a total of four basidiospores, while the other typically lacks spermogonia and produces two-celled promycelia with only two basidiospores. While transmission electron microscopy (TEM) has been used to examine aeciospores, aeciospore germination, and appressorium formation in *G. peckiana* (Swann and Mims 1991), there have been no detailed ultrastructural studies of either the teliospores or the sequence of events leading to basidiospore formation in the two endocyclic forms. In this paper we provide ultrastructural data on the four-spored form. The only information currently available on the teliospores and the events leading to basidiospore formation in this organism comes from line drawings included in the early light microscopic studies noted above.

Materials and methods

The specimens of *G. nitens* we examined came from infected southern-dewberry plants (*Rubus trivialis* Michx.) collected near the city of Nacogdoches in central eastern Texas. Infected shoots with leaves bearing sori were removed from plants and transported to the laboratory where some infected leaves were removed, and a razor blade was used to excise small pieces bearing sori to be used in the study of developing and mature teliospores. Other shoots were left in water overnight before the leaves were removed and used as sources of spores for the germination study described below. For the study of developing teliospores, leaf pieces were prepared for either scanning electron microscopy (SEM) or TEM using a standard glutaraldehyde–OsO_4 fixation procedure (Taylor and Mims 1991). Samples for SEM were processed according to the procedures of Enkerli et al. (1997). Following critical-point drying, samples were mounted on specimen stubs using conductive tape, sputter-coated with gold, and examined using a JEOL 6400 microscope operating at 15 kV. For TEM, thin sections of resin-embedded samples were cut using a Reichert ultramicrotome equipped with a diamond knife, collected on slot grids, and allowed to dry on formvar-coated aluminum racks (Rowley and Moran 1975). Sections were post-stained with uranyl acetate followed by lead citrate, and examined using a Zeiss 902A transmission electron microscope operating at 80 kV. For light microscopy (LM) of resin-embedded samples, sections approximately 1 μm in thickness were cut using a diamond histo-knife, collected on glass microscope slides, stained with toluidine blue O, and examined and photographed using bright-field microscopy.

To study the details of teliospore germination and basidium/basidiospore formation, leaves bearing sori were placed in drops of water on glass microscope slides and tapped with the end of a wooden applicator stick to dislodge spores from sori. The leaves were discarded and the slides bearing the hydrating spores then were placed in a moist chamber on a laboratory bench at approximately

Figs. 4–7. Scanning electron micrographs showing sori and teliospores of *Gymnoconia nitens*. Fig. 4. A young, circular sorus filled with spores. Scale bar = 100 μm. Fig. 5. A small portion of an older, elongated sorus. Scale bar = 40 μm. Fig. 6. Spores within a sorus (note their angular nature). Scale bar = 20 μm. Fig. 7. A higher magnification view of the tiny warts present on spores. Scale bar = 10 μm.

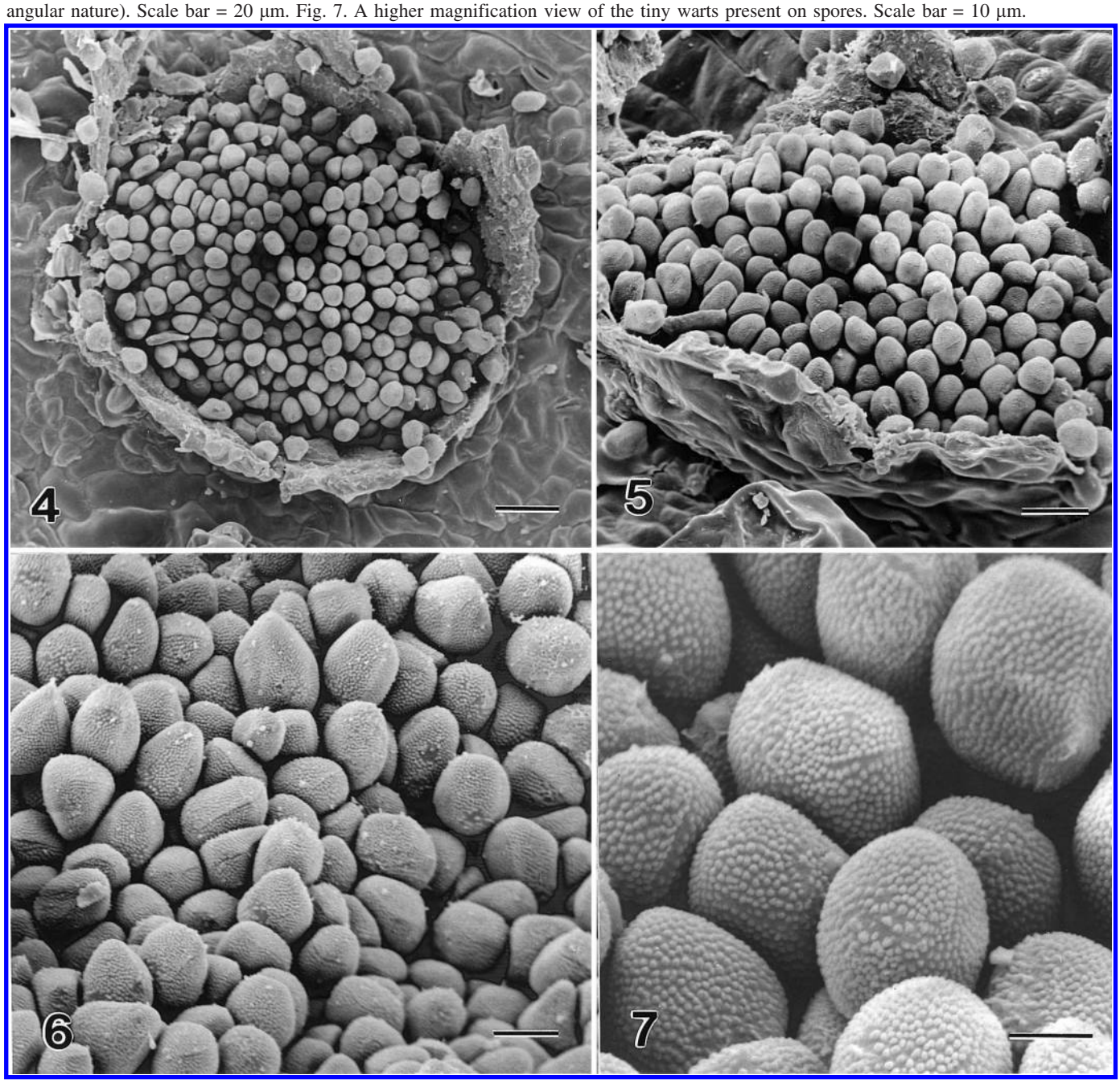

23 °C. At 1, 2, 4, 6, and 8 h time intervals after being placed in water, a gentle stream of water from a plastic squeeze bottle was used to wash samples off the slides and into the center of a Kimwipe® tissue spread over and pushed into the mouth of a small beaker. A piece of thread was used to tie off the depressed end of the tissue in which the samples accumulated, and the remainder of the tissue was cut off and discarded. The resulting small bag was used to carry the samples through fixation, dehydration, and resin embedment. Once samples had been completely infiltrated with 100% resin, the thread was removed from the bag, its contents were teased into a small amount of fresh 100% resin on a 25 mm × 75 mm plastic Permanox® cell culture slide and an identical slide was placed on top of the resin. Following resin polymerization, the lower slide was removed by sliding a razor blade between it and the thin layer of resin adhering to the upper slide. The samples in the resin layer were examined using LM, and small rectangular pieces of resin-infiltrated samples were excised using a pointed-tip blade, glued on blank resin blocks, and trimmed with a razor blade to produce block faces for thin-sectioning (Mims et al. 1988). Thin sections were cut, collected, post-stained, and examined using TEM, as described above.

Figs. 8–14. Light (Figs. 8, 9, 13, and 14) and transmission electron micrographs (Figs. 10–12) illustrating details of teliospore formation and promycelium formation in *Gymnoconia nitens*. Fig. 8. A low magnification view of a portion of a sectioned sorus showing chains of developing spores. Scale bar = 100 μm. Fig. 9. Slightly higher magnification view of sporogenous cells (asterisks) and chains of developing and mature teliospores. Developing and mature spores in which two nuclei are visible are shown at the arrowheads. Scale bar = 40 μm. Fig. 10. A section showing a binucleate sporogenous cell (SC) and a binucleate teliospore initial (TI) with nuclei shown at N. Scale bar = 1.5 μm. Fig. 11. A section showing the two nuclei (N) of a young teliospore (T) with a disjunctor cell visible at DC. Scale bar = 1.5 μm. Fig. 12. A mature teliospore in which both nuclei (N) are visible. Scale bar = 1.5 μm. Figs. 13 and 14. Flat-embedded promycelia with nuclei visible at the arrows. Scale bars = 50 μm.

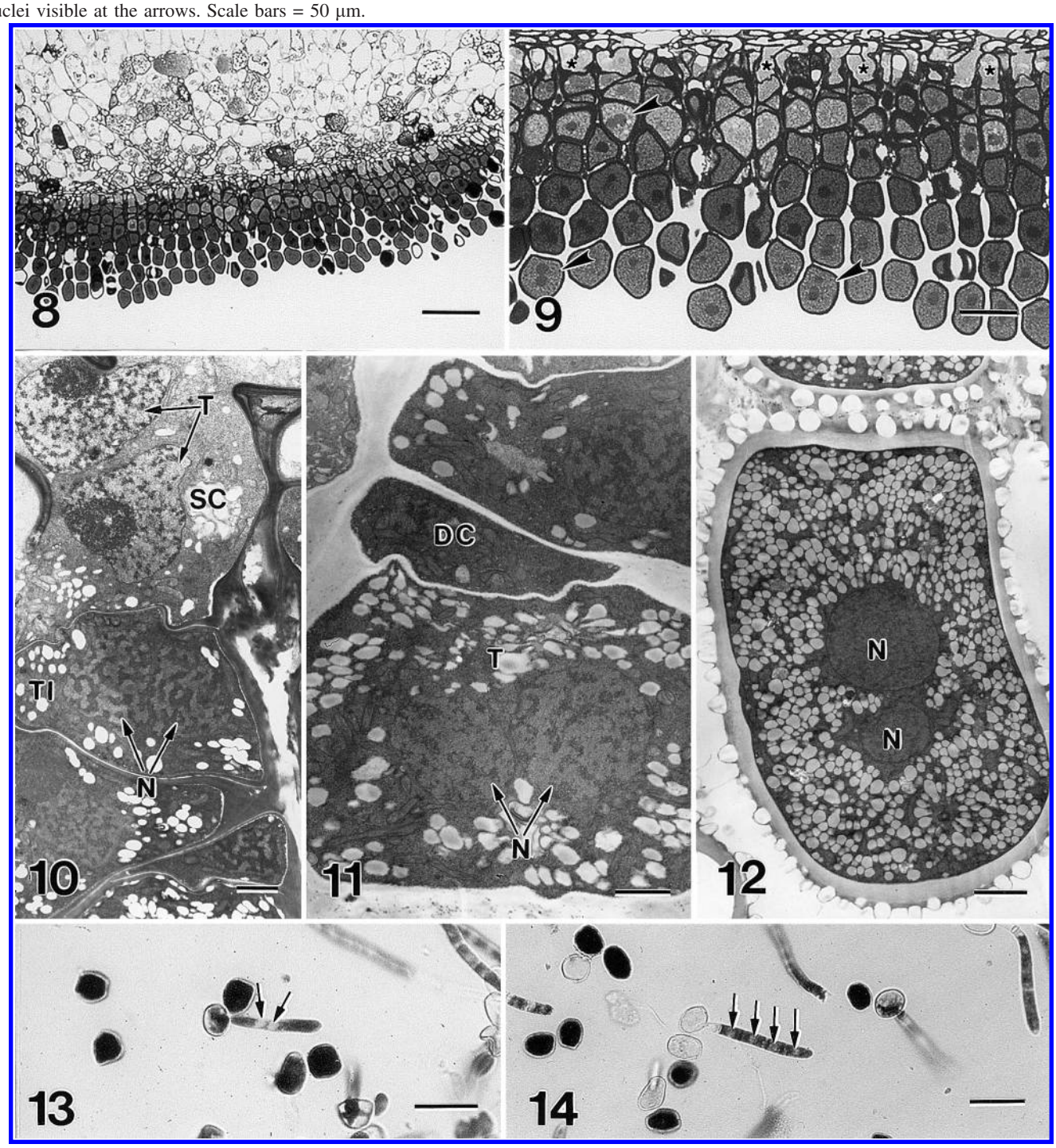

Results

Sori of *G. nitens* almost completely covered the undersides of most infected leaves of *R. trivialis* (Figs. 1–3). Although young sori were small with roughly spherical mouths (Fig. 4), older sori were much larger and usually very elongated structures (Figs. 2, 3, and 5). Each sorus was packed with caeomatoid teliospores that possessed dis-

Figs. 15–18. Transmission electron micrographs of teliospores of *Gymnoconia nitens*. Fig. 15. A hydrated spore prior to the emergence of a germ tube with the spore nuclei shown at N, lipid bodies at L, and germ pore regions at the arrowheads. Fig. 16. A hydrated spore with more prominent germ-pore regions (arrowheads) than in Fig. 15. Only one of the two spore nuclei (N) is visible. Fig. 17. An early stage in teliospore germination where the germ tube (GT) or developing promycelium had just emerged from a germ-pore region. Fig. 18. A developing promycelium (arrow) where the nuclei (N) are still in the spore. Scale bars = 1.5 μm.

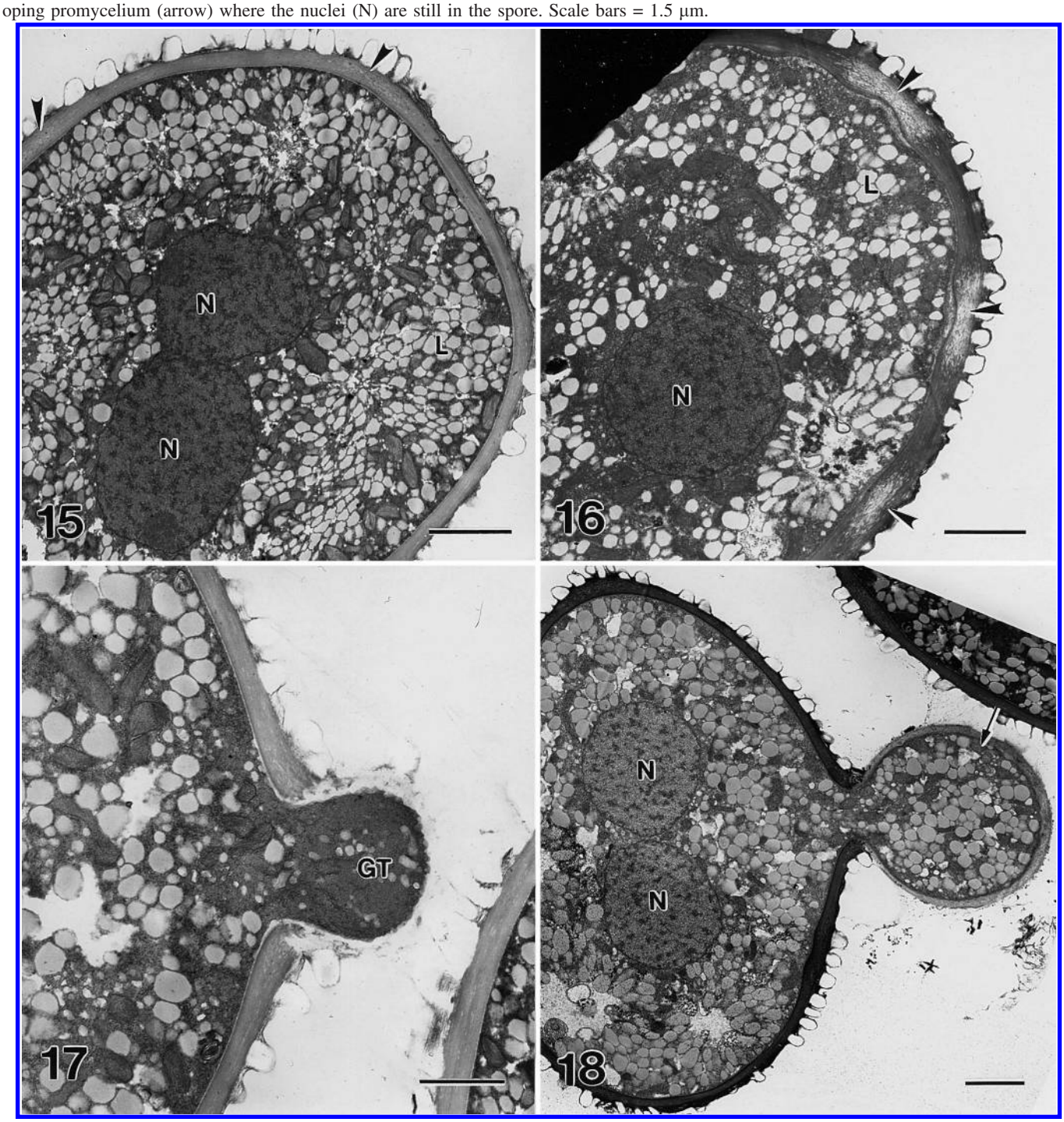

tinctly angular surface features when viewed using SEM (Fig. 6). Most spores measured 17–18 μm × 20–21 μm and were covered with tiny, rounded warts (Fig. 7).

LM of sections of resin-embedded sori revealed chains of teliospore initials and developing teliospores that arose from a basal layer of sporogenous cells (Figs. 8 and 9). Each sporogenous cell was binucleate and gave rise to a series of binucleate teliospore initials (Fig. 10), each of which subsequently divided to form a larger apical teliospore and a smaller basal disjunctor cell (Fig. 11). Examination of serial sections confirmed that each young teliospore was binucleate. We found no evidence of karyogamy during either teliospore formation or maturation, and the mature spores we examined were binucleate (Fig. 12).

Figs. 19–23. Transmission electron micrographs of nuclei in promycelia of *Gymnoconia nitens*. Fig. 19. A developing promycelium containing two nuclei (N) with a portion of the parent teliospore visible (arrow). Scale bar = 1.5 μm. Fig. 20. A higher magnification view of one of the two nuclei (N) of a promycelium with the spindle-pole body visible at the arrowhead. Scale bar = 0.5 μm. Fig. 21. The synchronous division of the two nuclei (N) of a promycelium. Scale bar = 1 μm. Fig. 22. An example of a mitotic nucleus with both the spindle apparatus (SA) and the spindle-pole bodies (arrowheads) visible. Scale bar = 0.5 μm. Fig. 23. A section showing three cells of a four-celled promycelium with two septa visible (arrowheads) along with a single nucleus (N) in each cell. Scale bar = 1.5 μm.

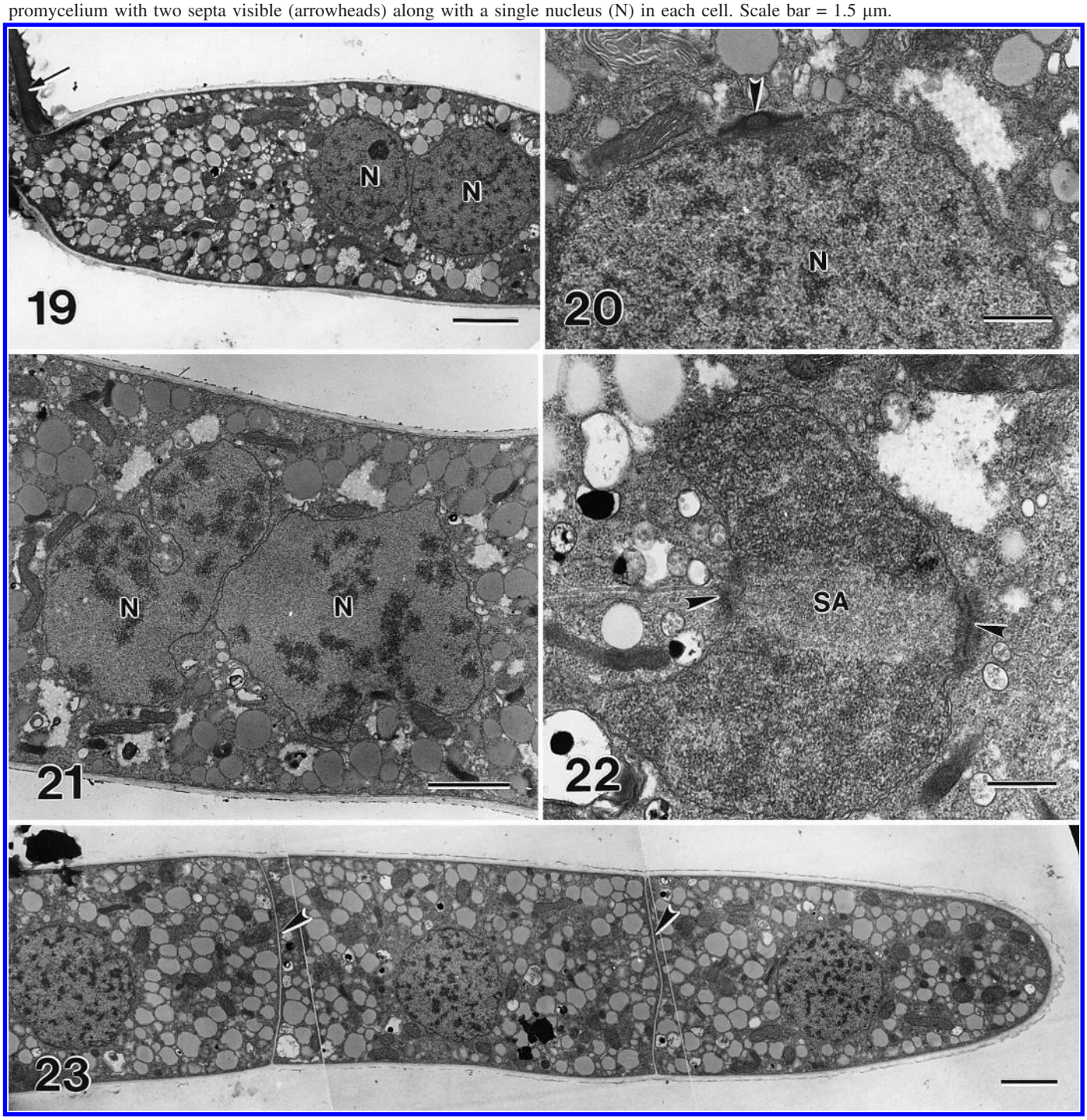

The use of flat-embedded samples greatly facilitated the study of the events occurring during teliospore germination and basidium/basidiospore formation in the four-celled form of *G. nitens*, as we could examine a particular sample first with LM and then with TEM. With the exception of ungerminated spores, we could see nuclei at the LM level in our flat-embedded samples (Figs. 13 and 14). This proved to be extremely valuable in elucidating details of nuclear behavior during basidium and basidiospore formation. To determine the nuclear condition in ungerminated spores, we examined serial sections of a number of spores and found that they also were binucleate (Fig. 15).

Fig. 24–28. Light (Fig. 24) and transmission electron micrographs (Figs. 25–28) of basidiospore development in *Gymnoconia nitens*. Fig. 24. A maturing promycelium with four developing basidiospores (arrows). Scale bar = 50 μm. Fig. 25. The apical cell of a promycelium with a developing sterigma (S) with the nucleus is visible at N. Fig. 26. The tapered tip (arrowhead) of an elongating sterigma (S). Fig. 27. A developing basidiospore (BS) at the tip of a sterigma (S) where the nucleus has not yet entered the spore. Fig. 28. A maturing basidiospore containing a mitotic nucleus (N). Scale bars = 1.5 μm for Figs. 25–28.

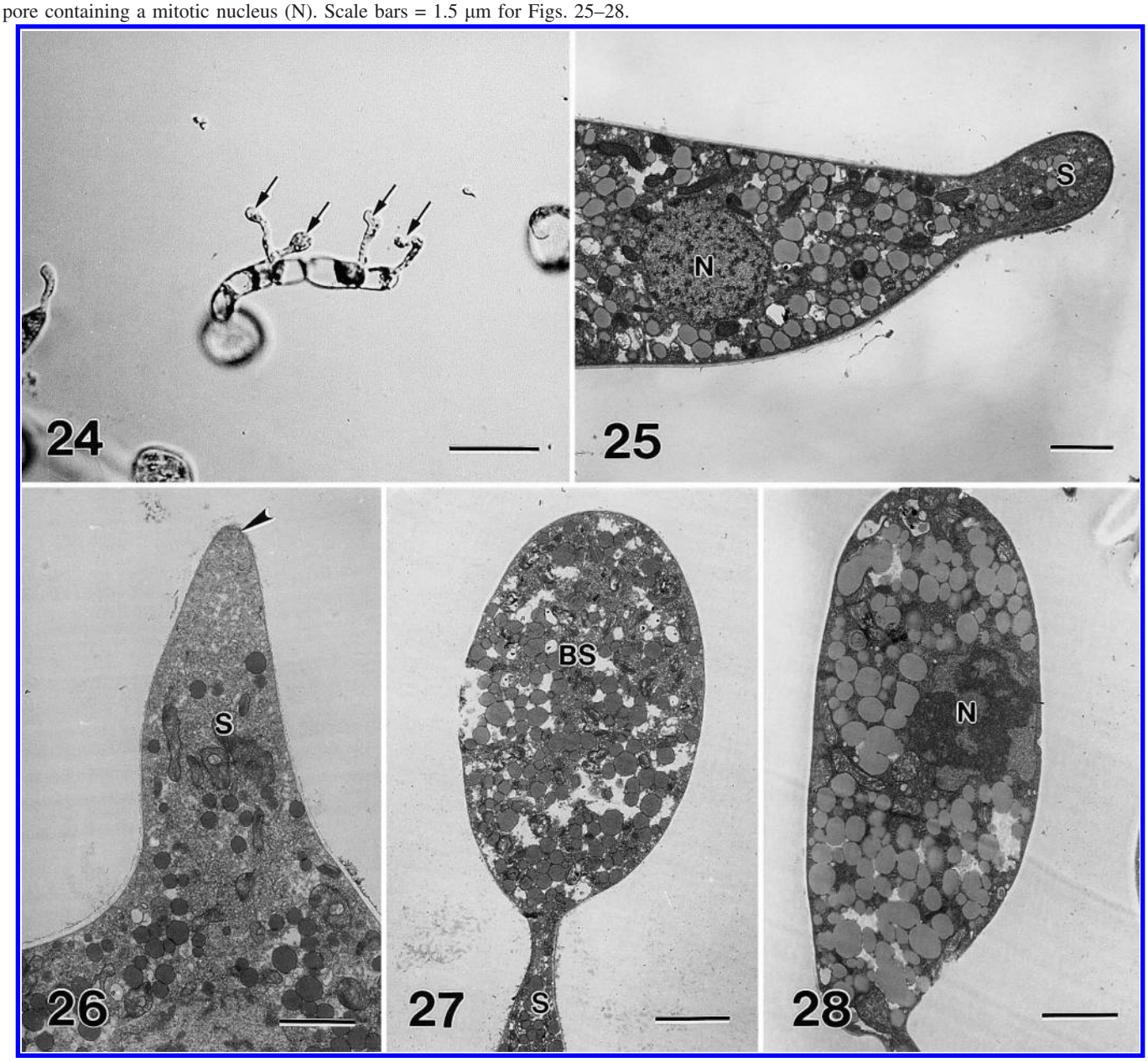

Early stages of germ-tube emergence were common at the 4 h sampling period. However, some spores did not begin to germinate until 6 or even 8 h after the onset of hydration and many showed no evidence of germination even at 8 h. Each teliospore was packed with lipid bodies and possessed a number of germ pore regions in its wall (Figs. 15 and 16). Upon germination, a single germ tube emerged from each spore (Figs. 17 and 18). Most of the spore cytoplasm as well as both nuclei moved into the germ tube, which will be referred to here as the promycelium. Fully elongated promycelia were somewhat variable in length but most measured 80–105 μm. The two nuclei eventually became situated near the middle of a promycelium (Fig. 19). A duplicated spindle-pole body was present on the surface of each nucleus (Fig. 21). The two nuclei divided synchronously (Figs. 21 and 22), and the four resulting daughter nuclei became distributed more or less evenly along the length of the promycelium. In most instances, four septa then developed to divide the promycelium into four uninucleate cells, three of which are visible in Fig. 23. Although some four-celled promycelia were observed as early as 6 h after the onset of hydration, they were much more common at 8 h. By 8 h, basidiospores had also begun to develop on many promycelia (Fig. 24). The first cell to give rise to a sterigma was typically the apical cell (Fig. 25). The tip of a maturing sterigma became distinctly pointed (Fig. 26) prior

to forming a basidiospore (Fig. 27). Most of the cytoplasm and the nucleus of the parent cell eventually migrated into the basidiospore. Once in the spore the nucleus underwent mitosis (Fig. 28).

Discussion

The most significant finding in this study relates to the fact that while the four-celled form of *G. nitens* forms promycelia and basidiospores that are morphologically identical to those produced by most other rust fungi, it apparently does so without undergoing sexual reproduction. The asexual production of promycelia and basidiospores in rust fungi has been reported previously in a few microcyclic species (Hiratsuka and Sato 1982), but this is the first time the phenomenon has been demonstrated with TEM. TEM has previously proven to be a valuable method for elucidating details of the nuclear cycle in rust fungi, and has been used to document the sites of nuclear fusion and meiosis in a number of rust fungi. Based upon reports of synaptonemal complexes in the nuclei of young rust teliospores (Mims 1977, 1981; Boehm and Bushnell 1992; Boehm et al.1992; Mims et al. 1996; Mims and Richardson 2005), it appears that both karyogamy and prophase I of meiosis occur in young teliospores. Meiosis then appears to be arrested in late prophase and not completed until after the nucleus has migrated into the promycelium (see O'Donnell and McLaughlin 1981*a*, 1981*b*) that eventually arises from a germinating teliospore. In the four-celled form of *G. nitens* examined here, we found no evidence that either karyogamy or meiosis occurred during the formation, maturation, or germination of the caeomatoid teliospores. Both developing and mature teliospores were found to be binucleate and, following teliospore germination, both nuclei migrated into the promycelium where they divided mitotically to yield four nuclei. This conforms to the type II behavior described by Hiratsuka and Sato (1982). Overall, Hiratsuka and Sato (1982) described a total of eight types of nuclear behavior in rust teliospores and basidia, which they referred to as types I–VIII. They stated that the nuclei in species exhibiting type II behavior were haploid, but provided no direct evidence to support this statement. Here we should note that monokaryotic strains of certain holobasidiomycetes (see Stahl and Esser 1976) have also been reported to form basidiospores without karyogamy and meiosis.

Although various workers have reported some minor size and possible color differences between the caeomatoid teliospores of *G. nitens* and the aeciospores of *G. peckiana*, the only reliable way to differentiate between these two types of spores is to germinate them. On inductive surfaces such as pieces of dialysis membrane, an aeciospore of *G. peckiana* gives rise to very short germ tube whose tip quickly differentiates into a swollen appressorium (Swann and Mims 1991), while as described in this study, the germ tube or promycelium that arises from a caeomatoid teliospore of *G. nitens* eventually forms basidiospores.

The overall process of teliospore formation in *G. nitens* appears to be identical to that of aeciospore formation in other rust fungi. As described by various other workers (see Littlefield and Heath 1979), the base of an aecium is lined with binucleate mother cells that give rise to a succession of binucleate sporogenous cells. Each sporogenous cell divides to form a small binucleate basal cell known as a disjunctor cells that eventually dies and a larger binucleate cell that develops into an aeciospore.

References

Boehm, E.W.A., and Bushnell, W.R. 1992. An ultrastructural pachytene karyotype for *Melampsora lini*. Phytopathology, **82**: 1212–1218.

Boehm, E.W.A., Wenstrom, J.C., McLaughlin, D.J., Szabo, L.J., Roelfs, A.P., and Bushnell, W.R. 1992. An ultrastructural pachytene karyotype for *Puccinia graminis* f. sp. *tritici.* Can. J. Bot. **70**: 401–413. doi:10.1139/b92-054.

Clinton, G.P. 1893. Orange rust of raspberry and blackberry. Ill. Agr. Exp. Sta. Bull. **29**: 273–300.

Cummins, G.B., and Hiratsuka, Y. 2003. Illustrated genera of rust fungi. 3rd ed. APS Press, St. Paul, Minn.

Dodge, B.O. 1924. Uninucleated aecidiospores in *Caeoma nitens*, and associated phenomena. J. Agric. Res. **28**: 1045–1058.

Enkerli, K.M., Hahn, M.G., and Mims, C.W. 1997. Ultrastructure of compatible and incompatible interactions of soybean roots infected with the plant pathogenic oomycete *Phytophthora sojae.* Can. J. Bot. **75**: 1493–1508. doi: 10.1139/b97-864.

Hiratsuka, Y., and Sato, S. 1982. Morphology and taxonomy of rust fungi. *In* The rust fungi. *Edited by* K.J. Scott and A.K. Chakravorty. Academic Press, New York. pp. 1–36.

Kleiner, W.C., and Travis, J.W. 1991. Orange rust. *In* Compendium of raspberry and blackberry diseases and insects. *Edited by* M.A. Ellis, R.H. Converse, R.N. Williams and B. Williamson. APS Press, St. Paul, Minn. pp. 26–28.

Kunkel, O. 1913. The production of a promycelium by the aeciospores of *Caeoma nitens* Burrill. Bull. Torrey Bot. Club, **40**: 361–366. doi:10.2307/2479880.

Kunkel, O. 1914. Nuclear behavior in the promycelia of *Caeoma nitens* Burrill and *Puccinia peckiana* Howe. Am. J. Bot. **1**: 37–46. doi:10.2307/2434959.

Kunkel, O. 1916. Further studies of the orange rusts of *Rubus* in the United States. Bull. Torrey Bot. Club, **43**: 559–567. doi:10.2307/2479608.

Littlefield, L.J., and Heath, M.C. 1979. Ultrastructure of rust fungi. Academic Press, New York.

Mims, C.W. 1977. Ultrastructure of teliospore germination in the cedar apple rust fungus *Gymnosporangium juniperi-virginianae.* Can. J. Bot. **55**: 2319–2329. doi:10.1139/b77-263.

Mims, C.W. 1981. Ultrastructure of teliospore germination and basidiospore formation in the rust fungus *Gymnosporangium clavipes.* Can. J. Bot. **59**: 1041–1049. doi:10.1139/b81-142.

Mims, C.W., and Richardson, E.A. 2005. Light and electron microscopy of teliospores and teliospore germination in the rust fungus *Coleosporium ipomoeae.* Can. J. Bot. **83**: 451–458. doi:10.1139/b05-020.

Mims, C.W., Richardson, E.A., and Timberlake, W.E. 1988. Ultrastructural analysis of conidiophore development in the fungus *Aspergillis nidulans* using freeze-substitution. Protoplasma, **144**: 132–141. doi:10.1007/BF01637246.

Mims, C.W., Liljebjelke, K.A., and Covert, S.F. 1996. Ultrastructure of telia and teliospores of the rust fungus *Cronartium quercuum* f. sp. *fusiforme.* Mycologia, **88**: 47–56. doi:10.2307/3760783.

Newcombe, F.C., and Galloway, B.T. 1890. Perennial mycelium of the fungus of the blackberry rust. J. Mycol. Plant Pathol **6**: 106–107.

O'Donnell, K.L., and McLaughlin, D.J. 1981*a*. Ultrastructure of

meiosis in the hollyhock rust fungus, *Puccinia malvacearum*. I. Prophase I – prometaphase I. Protoplasma, **108**: 225–244. doi:10.1007/BF02224421.

O'Donnell, K.L., and McLaughlin, D.J. 1981*b*. Ultrastructure of meiosis in the hollyhock rust fungus, *Puccinia malvacearum*. II. Metaphase I – telophase I. Protoplasma, **108**: 245–263. doi:10.1007/BF02224422.

Olive, E.W. 1908. Sexual cell fusions and vegetative nuclear divisions in the rusts. Ann. Bot. (Lond.), **22**: 333–360.

Rowley, J.C., and Moran, D.T. 1975. A simple procedure for mounting wrinkle-free sections on formvar coated slot grids. Ultramicroscopy, **1**: 151–155. PMID:800684.

Stahl, U., and Esser, K. 1976. Genetics of fruit body production in some higher basidiomycetes. Mol. Gen. Genet. **148**: 183–197. doi:10.1007/BF00268384.

Swann, E.C., and Mims, C.W. 1991. Ultrastructure of freeze-substituted appressoria produced by aeciospore germlings of the rust fungus *Arthuriomyces peckianus.* Can. J. Bot. **69**: 1655–1665. doi:10.1139/b91-210.

Taylor, J., and Mims, C.W. 1991. Fungal development and host cell responses to the rust fungus *Puccinia substriata* var. *indica* in seedlings and mature leaves of susceptible and resistant pearl millet. Can. J. Bot. **69**: 1207–1219. doi:10.1139/b91-155.